JOURNAL OF MATERIALS SCIENCE **35** (2000) 4099–4107

Characterisation of microstructures in nickel based transition joints

J. D. PARKER, G. C. STRATFORD
Department of Materials Engineering, University of Wales, Swansea, UK
E-mail: j.d.parker@swansea.ac.uk

The microstructural changes occurring at the low alloy steel fusion line in nickel based transition welds are believed to be critical to the development of creep cavities and cracks. The progressive changes in Type I carbides observed following laboratory ageing at 625°C and from interrupted creep specimens tested at 590–625°C have been evaluated by optical and electron microscopy. In general, these carbides appear to be $M_{23}C_6$ type and grow in an approximately elliptical shape with the long dimension in the plane of the interface. The behaviour noted is in good general agreement with a cubic growth law and predictions made from laboratory results are in agreement with previous observations from plant welds. The accuracy of these predictions is such that measurements of carbides in service can be used to estimate an equivalent operating temperature.

1. Introduction

Filler metals with about 60% nickel were developed to weld creep resistant low alloy steel to austenitic stainless steel. The joints produced provide superior performance compared with piping welds manufactured using austenitic steel consumables [1]. However, operating experience at high temperature and pressure indicates that creep damage has been noted in nickel based welds at the low alloy steel fusion line. The development of this damage appears to be associated with time dependent changes in microstructure [1]. The present programme has therefore been carried out to study the effects of ageing on weldment microstructure. The current paper considers microstructural changes during laboratory heat treatment and creep tests, with work in subsequent reports studying the strain accumulation and damage noted during creep exposure.

2. Experimental procedures

An Inconel based transition joint was manufactured by butt welding a 2.25Cr-1Mo low alloy ferritic steel pipe to a Type 316 austenitic stainless steel pipe using Inco In182 nickel based weld metal. Both piping sections had an outside diameter of 350 mm and a wall thickness of 25 mm. The welding procedure adhered to British Standard BS.2633 [2] and the welding process was followed by a post weld heat treatment (PWHT) of 700°C for 3 hours. For the purposes of this programme, welds in this condition were defined as "as-received".

The weldment was subsequently used to fabricate creep specimens for a uniaxial creep testing programme [3] and the samples required for a heat treatment programme to examine the effects of thermal exposure on the microstructure and properties of the Inconel joints. This programme is described below.

2.1. Thermal exposure

This programme involved heat treating sections of weldment at a temperature of 625°C for up to 6000 hours. Specimens for the heat treatment programme were manufactured by sectioning the weldment into rectangular blocks. Each block had dimensions of approximately $15 \times 15 \times 60$ mm and contained the nickel based weld metal section at the centre of its length.

One block was metallographically examined in the as-received condition while the remaining blocks were coated in an oxidation inhibiting coating to reduce the effects of oxidation during the thermal exposure. These blocks were instrumented with calibrated Type-K thermocouples and placed into a CARBOLITE furnace pre-heated to 625°C. During the heat treatment programme, the specimen and furnace temperatures were regularly monitored. The blocks were allowed to soak in the furnace for 5 hours before the timing of the heat treatment process began. The first heat treated block was removed after 500 hours and subsequent blocks were then removed at 500 hour intervals up to a maximum of 6000 hours.

In addition, uniaxial creep tests at 590°C, 605°C and 625°C were interrupted at times ranging from 350 to 8600 hours and the specimens removed for metallographic preparation and microscopic examination.

2.2. Metallographic preparation

After removal from the furnace, each block was machined to give flat, square faces then hand ground with

60 and 120 grit papers to remove any effects of the machining process. The blocks were then prepared using standard grinding techniques to a flat ground finish using 1200 grit paper. This ground surface was then given an initial polish with 6 μm diamond polish. Subsequently a mirror finish was obtained using a 1 μm diamond polish and this was followed by a light etch with a 2% Nital etchant. The fine polish and etch procedure was repeated three times to ensure that the microstructure's image was clear and the structure at the weld interface was fully revealed.

In addition to the heat treated blocks, uniaxial cross weld creep specimens were examined after creep exposure to allow a comparison of microstructures for similar thermal exposures with and without an applied stress. Thus, square sectioned creep specimens [3] were prepared using a similar method to the heat treated blocks using a hand-held electric powered grinder/polisher and the same repeated polish/etch cycle.

2.3. Microscopy

Initial metallographic examination was undertaken using a light-optic microscope at magnifications up to 500×. However, the weld interface contained structures which required greater magnifications and thus electron microscopy was employed. Regions of interfacial precipitates were identified using the Scanning Electron Microscope (SEM) and were examined at a magnification of 5000×. This magnification was selected to give a balance between the requirement for clear images of interfacial microstructures at a size which made them measurable, and the need to get a reasonable number of precipitates on each frame to assess their distribution. Representative areas of interfacial precipitates were digitised using an OPTILAB image grabbing system. This allowed images of the interface to be acquired which could subsequently be enlarged digitally to enhanced the accuracy of the carbide size measurements. For each specimen, 6–8 images were selected and analysed. Each image was digitally enlarged to a size of 200 × 250 mm. Depending on the thermal exposure, each image could contain 10 to 50 Type I carbide particles. On each image, the size, number and distribution of the interfacial precipitates were measured and recorded. Size measurements were taken in both the major axis, M (parallel to the weld interface), and in the minor axis, m, (perpendicular to the weld interface).

2.4. Hardness testing

Vickers macrohardness measurements using a 20 kg load were undertaken in the 2.25Cr-1Mo parent metal regions of the heat treated blocks to investigate the material's tempering performance. Ten measurements were made on each sample and a mean average hardness was calculated. Microhardness measurements were also made across the weld interface. Traverses were performed with a 500 g load with measurements taken at 0.125 mm intervals.

2.5. Chemical analysis

Chemical analysis was performed using Energy Dispersive X-ray Spectroscopy (EDX) in association with the examination by SEM. Spot analyses were carried out to identify the composition of individual precipitates. In addition "area" analyses were undertaken with a view to establishing whether there was any trend in compositional variation between as-received and heat treated specimens. Each region examined was a $30 \times 30\,\mu$m square and analysis was performed at 200 μm intervals across the weld interface with the low alloy steel. A range of elements was detected but the analysis concentrated on the variation in chromium and nickel compositions.

3. Results

3.1. Weldment microstructure

A macro-photograph of the various microstructural regions present in the low alloy steel adjacent to the as-received weld is presented in Fig. 1. The IN182 weld metal is shown to the right of the figure, the weld heat affected zone (HAZ) in the centre and a region of ferritic base metal to the left. The Inconel weld metal displayed a predominantly cast structure with weld beads defined by the initial welding process.

The low alloy steel heat affected zone structure was approximately 2 mm in width. The microstructural region adjacent to the weld interface, consisted of a coarse grained microstructure, shown in Fig. 2a. This region accounted for approximately one fifth of the HAZ width. The remainder of the HAZ structure was predominantly fine grained bainite as shown in Fig. 2b. The outer limit of the HAZ consisted of a region of mixed microstructure in the form of an Inter Critical Zone (ICZ). This ICZ contained both fine grain bainitic and relatively large grained ferritic parent structure.

The parent 2.25Cr-1Mo low alloy steel base metal consisted of a structure of approximately 80% ferrite and 20% bainite structures with an average ferritic grain size of 17 μm, Fig. 2c.

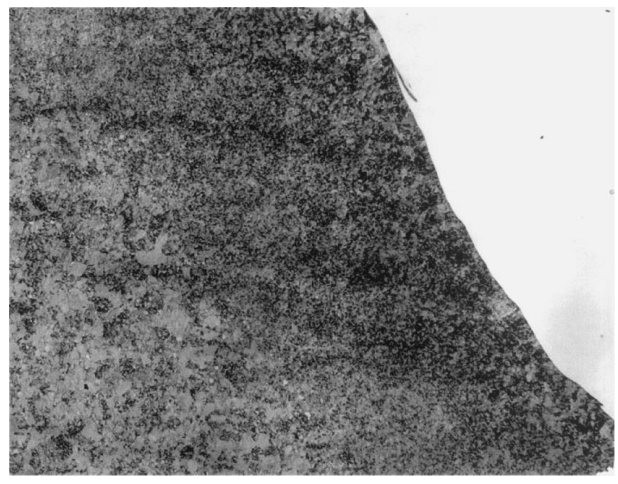

Figure 1 A macro-photograph of the various microstructural regions present in the low alloy steel adjacent to the as-received weld. The IN182 weld metal is shown to the right of the figure, the weld heat affected zone (HAZ) in the centre and a region of ferritic base metal to the left. (×25).

(a)

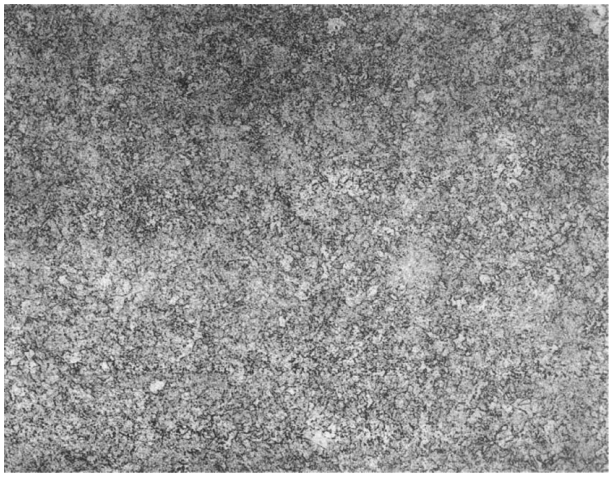

(b)

(c)

Figure 2 (a) A micrograph showing the coarse grained region of the low alloy steel heat affected zone adjacent to the weld interface. (×200) (b) A micrograph showing the fine grained bainitic region of the low alloy steel heat affected zone. (×200) (c) A micrograph of the outer limit of the heat affected zone consisting of a region of mixed microstructure in the form of an Inter Critical Zone (ICZ). (×200).

Following examination of the as-received weld using light microscopy, the specimen was placed in a JEOL 6100 SEM to characterise interfacial microstructures. The investigation, undertaken at magnifications up to 10,000×, concentrated on the 20 μm wide region of the low steel alloy adjacent to the weld interface.

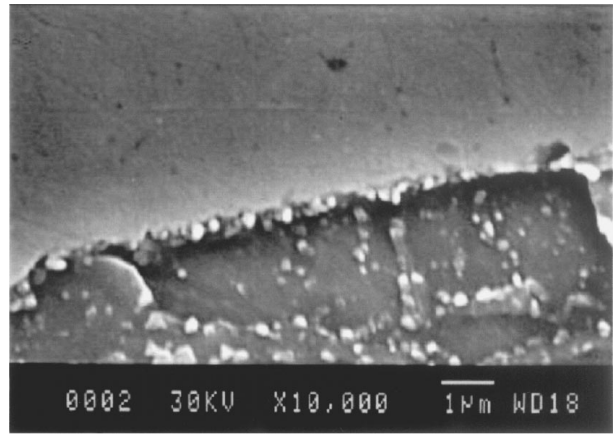

Figure 3 An election-micrograph detailing the precipitates observed in the interfacial region of the 2.25Cr-1Mo steel heat affecting zone of as-received welds.

The presence of precipitates was noted in the interfacial region of the 2.25Cr-1Mo steel HAZ of as-received welds, Fig. 3. However, these precipitates were small, diameters of the order of 0.1 μm, with a low density, i.e. the interparticle spacing was of the order of 0.5 μm. In addition, lath-like structures were noted on the interface. These were about 7–8 μm in thickness and appeared to be in regions of the HAZ which were adjacent to weld bead cusp regions.

3.2. Heat treated microstructures

Blocks were examined after 500, 1000, 1500, 2000, 2500, 3000, 3500, 4000, 4500, 5000, 5500 and 6000 hours exposure at 625°C. Under optical microscopic examination at magnifications of up to 500×, the microstructure of these specimens was little changed to that in the as-received condition. However, changes in microstructure were noted at the weld interface when examined using the Scanning Electron Microscope at magnifications of the order of 5000–10000×. In particular the thermal exposure had resulted in an array of precipitates at or near the interfacial region in the 2.25Cr-1Mo HAZ. These particles were of two distinct morphologies.

(i) A line of discrete spherical or lenticular particles ranging from 0.5–1.5 μm in size which appear at a distance of about 1 μm from the interface, Fig. 4a.
(ii) A lathe like structure, about 5–8 μm in width at a location parallel to the interface, Fig. 4b.

Indications from compositional analysis were that these precipitates were mainly $M_{23}C_6$ and M_6C carbide particles. Indeed the present observations are consistent with previous work which has described the structures in (i) as Type I carbides, and those in (ii) as Type II carbides [1, 4, 5].

3.3. Type I carbide size and distribution

Scanning Electron Microscopy examination of the heat treated blocks showed an increase in Type I carbide size with increased thermal exposure. In addition, the particles took on a distinct elongated lenticular appearance

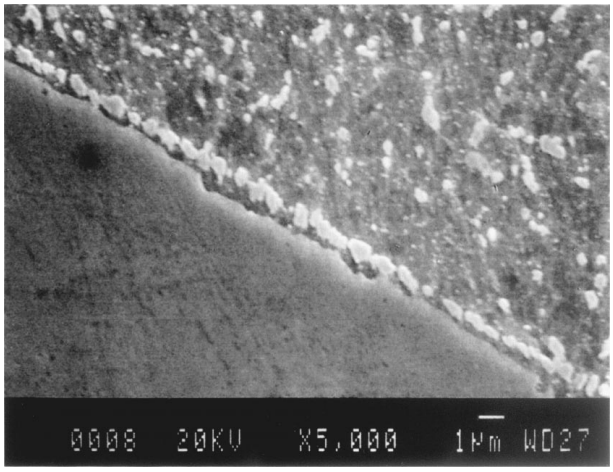

(a)

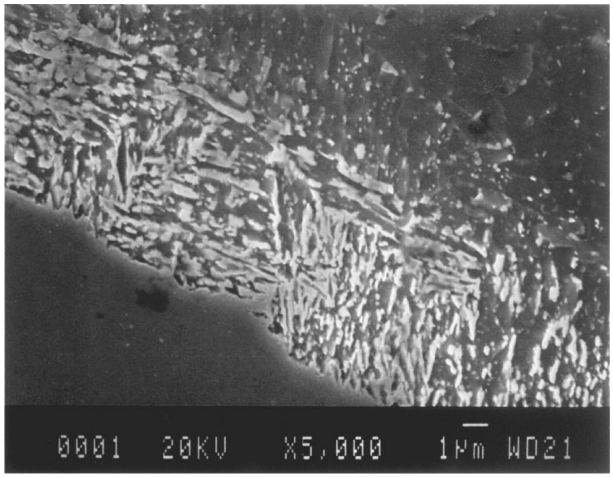

(b)

Figure 4 (a) An electron-micrograph showing the line of discrete spherical or lenticular particles which appear at a distance of about 1 μm from the weld interface. (b) An electron-micrograph detailing the lathe like structure observed in a location parallel to the weld interface.

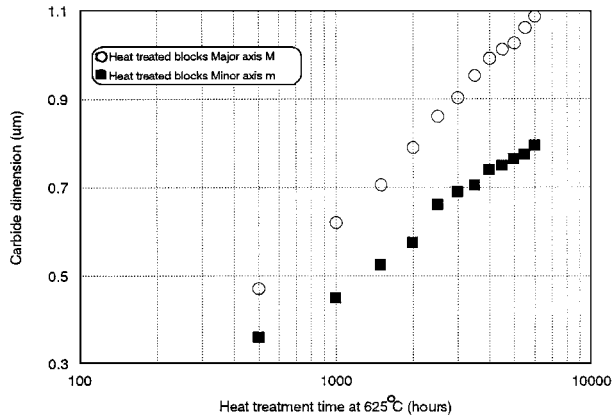

Figure 5 Variation in Type I carbide size in both the major, M, and minor, m, axis with ageing time for heat treatment blocks at 625°C.

which became more pronounced with ageing. Indeed at extended times, the Type I carbides were seen to develop aspect ratios in excess of 10 : 1 and linking up of carbides often occurred.

The results of these Type I carbide measurements from weldments after a range of heat treatment exposures are shown in Fig. 5. It can be seen that the particle dimensions increase with thermal exposure at 625°C.

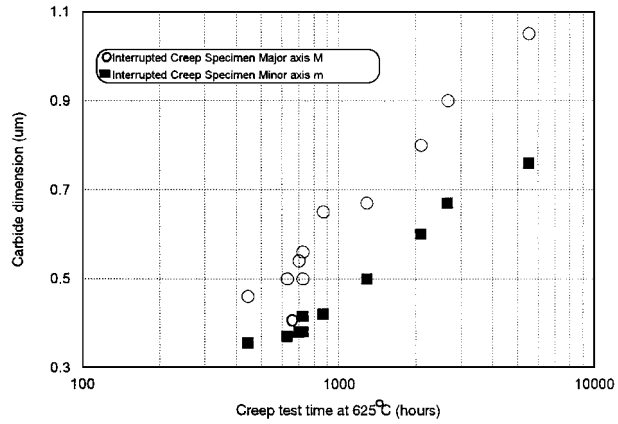

Figure 6 Variation in Type I carbide size in both the major, M, and minor, m, axis for observations taken from interrupted uniaxial cross weld creep specimens tested at 625°C.

An exposure of 6000 hours increased the size of the particles in the major axis direction from 0.47 μm (after 500 hours) to 1.085 μm and from 0.47 μm to 0.795 μm in minor axis direction.

In addition to the heat treated blocks, uniaxial creep specimens from the same weldment were examined in the SEM during regular test interruptions [3]. The major axis dimensions measured during the test life are shown in Fig. 6 and were seen to increase in a similar manner to those for the heat treated blocks, Fig. 5. In addition to carbide size other factors were noted and calculated:

(i) Carbides per unit length of interface:

$$\text{Carbides/unit length, } \rho = \frac{C}{L} \tag{1}$$

where C is the number of carbides on the section and L is the length of the section.

(ii) Interparticle spacing:

$$\text{Carbide Spacing } \varphi = \frac{(L - C \cdot M)}{(C - 1)} \tag{2}$$

where M is the average major axis carbide size.

The variation of carbide density in the interfacial region with exposure time from 500 to 6000 hours at 625°C is presented in Fig. 7. The number of carbides per unit length initially increased rapidly before reaching a peak

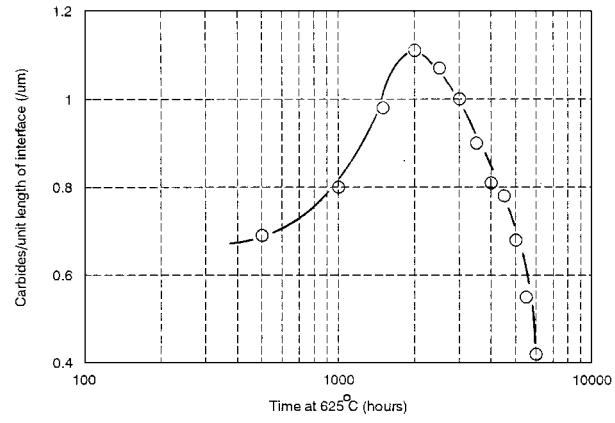

Figure 7 Variation in the number of Type I carbides per unit length of interface with time for observations taken from heat treated blocks.

of about 1.1 per μm for exposures of 2000 hours. The number of carbides per unit length then decreased up to times of 6000 hours. as the carbides linked and coalesced along the weld interface.

3.4. Type II carbide size and distribution

Type II carbides arrays were predominantly associated with the 2.25Cr-1Mo metal HAZ regions adjacent to the bead cusp regions in the Inconel weld metal. The structure was feathery and lath-like and was wider than the line of Type I carbides, often by a factor of 15 times, ie. a Type II carbide band thickness of about 8 μm was typical. The prolonged thermal exposure tended to make the Type II lath structure more diffuse. Indeed, for exposures in excess of 4000 hours no lath structures were apparent.

3.5. Hardness changes with thermal exposure

Hardness changes with ageing were assessed using macrohardness measurements. It can be seen in Fig. 8 that the parent material had an average initial hardness in the as-received condition of about 190 Hv. The hardness decreased as the exposure at 625°C increased so that after 6000 hours exposure the parent metal hardness had reduced to about 135 Hv. In the as-received condition, the weld metal had a hardness of about 200 Hv, Fig. 9. The hardness increased to 225 Hv at the weld interface before dropping across the HAZ to a base metal value of 190 Hv. Tests on a weldment which had been exposed at 625°C for 1000 hours showed a weld metal hardness of 210 Hv. A peak of 250 Hv was observed at the interface before the hardness dropped steeply to a near constant value of 175 Hv in the HAZ before dropping again to a value of 165 in the parent metal. Exposures of 3000 and 6000 hours showed similar characteristics. Weld metal hardnesses were about 210–220 with distinct hardness peaks observed at the weld interface. The 3000 hour specimen had a peak interface hardness of 255 Hv while the 6000 hour specimen had a peak interface hardness of 305 Hv. In both cases the hardness dropped rapidly in the coarse grained HAZ to about 150 Hv. Hardness values then rose to about 160 Hv in the fine grained HAZ before dropping to 150 Hv and 135 Hv for the 3000 hour and 6000 hour specimens respectively.

3.6. Chemical analysis

Chemical analysis was performed on heat treated blocks in the as-received and 6000 hour heat treated conditions. Figs. 10a and b show the variation in chromium and nickel composition across the weld interface. It can be seen that the changes in chemical composition of chromium and nickel after an exposure of 6000 hours were minimal with both specimens showing levels similar to initial values.

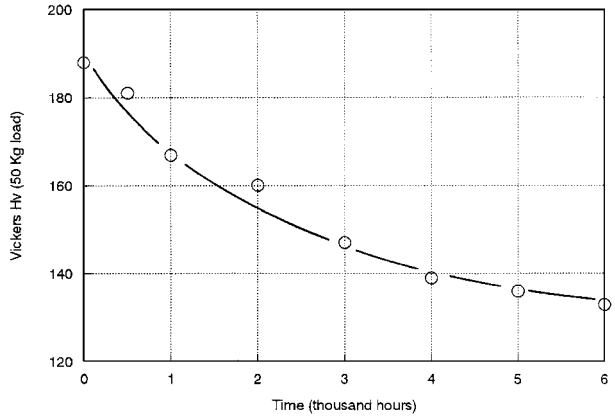

Figure 8 The variation in hardness with tempering time for 2.25Cr-1Mo parent metal.

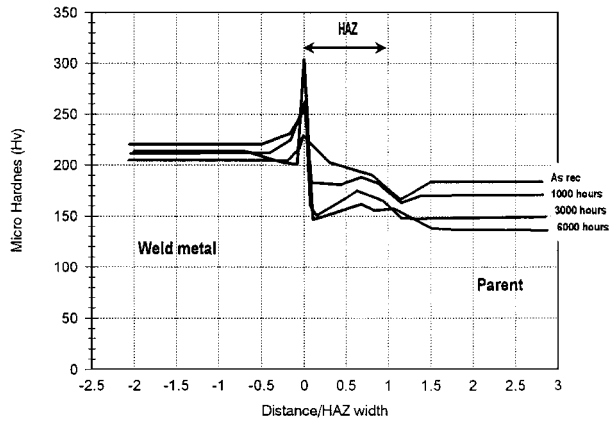

Figure 9 Microhardness traverses across the weld interface of Nickel-based weldments after heat treatment at 625°C.

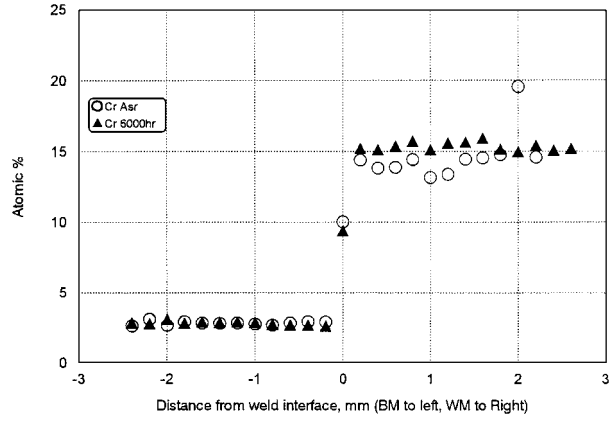

(a)

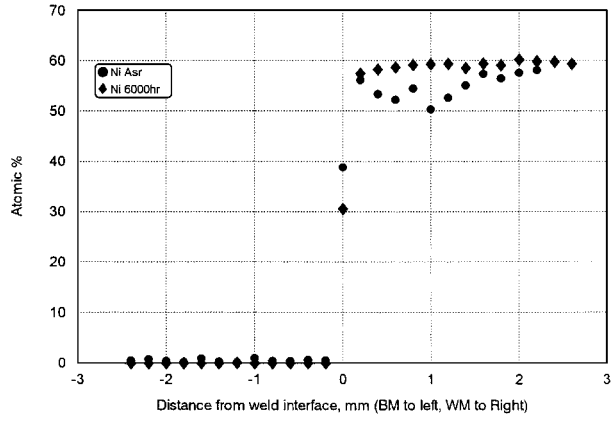

(b)

Figure 10 (a) The variation in Chromium content across the weld interface. (b) The variation in Nickel content across the weld interface.

4. Discussion

4.1. Microstructure

The examination of the as-received microstructure showed there to be Type I interfacial carbides present after the initial manufacture and PWHT processes. Thus, these structures, which have been linked to the low ductility failure of service welds [7], are present, albeit at a small size and low level, directly after weld manufacture and do not necessarily need in-service thermal exposure to be developed. However, the level of interfacial Type I carbides present was very low compared to that seen in specimens which had prolonged thermal exposure during heat treatment. While the as-received weld had undergone a thermal exposure in the form of post-weld heat treatment of 700°C for 3 hours, this did not result in significant carbide growth, Fig. 3. Therefore, carbides sizes remained of the order of 0.1 μm compared to carbides sizes 10 times larger following heat treatment at 625°C for several thousand hours.

Typical Type I carbides are shown in Fig. 4a. Initial work by Nicholson [6] reported similar Type I carbide structures in Inconel based transition joints. The measurements and subsequent analysis in the work of Nicholson were based on a single diameter measurement, d, ie. it was assumed that the particles were spherical. However, it is clear from the observations in the current work that the Type I carbides develop a lenticular geometry with the particle major axis lying parallel to the weld interface. The degree of elongation from a basic spherical particle shape can be observed in Fig. 11. This figure shows the change in Type I carbide size with exposure time for both heat treated blocks and observations taken from interrupted uniaxial creep specimens using the same weldment tested at 625°C. While it can be seen in this figure that the particles grow in both the major axis, M, and the minor axis, m, the rates of growth for each orientation were different. This indicates that the carbide particles become elongated with time, i.e. the particles grew more in the major axis along the interface than the minor axis over the same time period. Fig. 11 also shows that a weld interface under applied stress, such as a uniaxial test specimen and thus a service component, exhibits the same growth characteristic to that of heat treated block under zero loads. Thus, for the present heat treatment conditions it appears that applied stress has little effect on the growth characteristic of Type I carbides.

The observation that Type I carbides grow into particles with non-spherical geometries has also been noted by Viswanathan *et al.* [7] who analysed scanning electron micrographs from ex-service samples from 6 fossil fuel power plants. These workers noted that the use of structural parameters such as the major, M, and minor, m, axis of carbides could be used as a means of estimating service temperatures of components in service by relating size to thermal exposure.

It is generally accepted that during exposure at elevated temperatures, the growth of carbides can be simply described by a Wagner-Lifshitz [8, 9] type relationship of the form:

$$D^3 = D_o^3 + Bt \tag{3}$$

where D is the carbide size at time t, D_o is the carbide size at $t = 0$ and B is a constant.

Thus, if the carbide size at $t = 0$ is very small compared to the size at time t, the relationship becomes:

$$D^3 = B't \tag{4}$$

As B' is a temperature dependent constant, the relationship for carbide growth is more generally expressed as:

$$D^3 = k \cdot t \cdot \exp(-Q_g/RT) \tag{5}$$

where Q_g is the apparent activation energy for carbide growth, T is the exposure temperature, k is a constant and R is the gas constant (8.314 J/mol/K).

Consideration of Type I carbide measurements from both heat treated blocks and interrupted uniaxial creep specimens from the same weld indicates that data can be represented by Equation 5 for major, M, and minor, m, orientations, Fig. 12. From these relationships a value of $Q_g = 279$ KJ/mol was calculated for growth in the major axis and a value of 257 KJ/mol was calculated for growth in the minor axis. Given the effects of experimental scatter which accompanies measurements involving such small particles, these values of activation

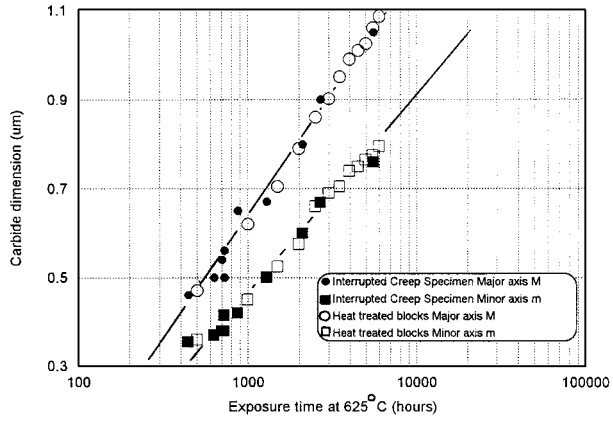

Figure 11 Variation in Type I carbide size in both the major axis, M, and minor axis, m, with time for observations taken from heat treated blocks and from uniaxial cross weld creep specimens 625°C.

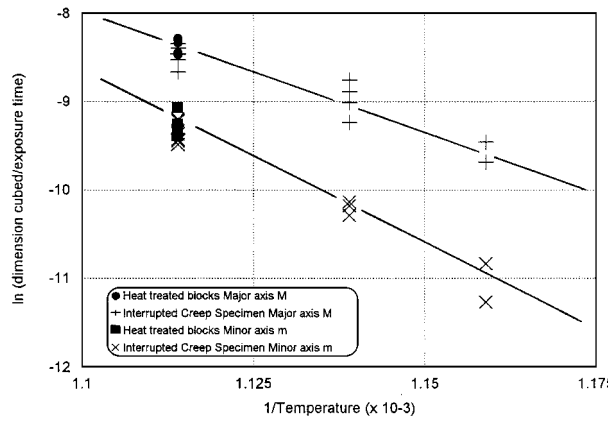

Figure 12 Temperature dependence of Type I carbide growth comparing data from heat treatment blocks exposed at 625°C with results from creep tests at 590°C, 605°C and 625°C.

energy are considered to be very similar. These values are also similar to those from other work [6] and are consistent with the required energy for thermally activated diffusional processes, such as volume diffusion.

Hence, using Equation 5, experimental values of D, t and T for both major and minor axes can be combined with appropriate activation energy vales to determine values of the constant k. Thus, for the major axis, $k = 1.199 \times 10^9\ \mu\text{m mol}\ Kt^{-1}J^{-1}$ and for the minor axis m, $k = 1.162 \times 10^{12}\ \mu\text{m} \cdot \text{mol} \cdot K \cdot t^{-1}J^{-1}$.

It is now possible to generate expressions which describe the growth of Type I interfacial carbides, based on a simple cubic Wagner-Lifshitz law and assuming negligible particle size at the start of thermal exposure as:

Major axis

$$M = 1.199 \times 10^9 \exp(-277 \times 10^3/RT)t \qquad (6)$$

Major axis

$$m = 1.162 \times 10^{12} \exp(-259 \times 10^3/RT)t \qquad (7)$$

Values of time and temperature were used with Equations 6 and 7 to generate curves predicting the Type I carbide growth behaviour. The curves produced were compared to other published relationships [6, 7] in Fig. 13. This figure shows a comparison of Type I carbides dimensions at 625°C over a 6000 hour time period calculated using Equations 6 and 7 above with estimates made from the models of Viswanathan *et al.* [7] and Nicholson [6]. Also shown are experimental data points from the current heat treatment programme. It can be seen that predictions made using the model developed from this programme and the Viswanathan model are in reasonable agreement with the experimental measurements. However, the work by Nicholson predicts dimensions which are smaller by a factor of 2 or more than the other models and the experimental observations.

Having a reliable model for Type I carbide growth allows calculations to be made which shows the growth characteristics of Type I carbides over range of times and temperatures which in turn may be applied to observations from ex-service joints to provide an estimate

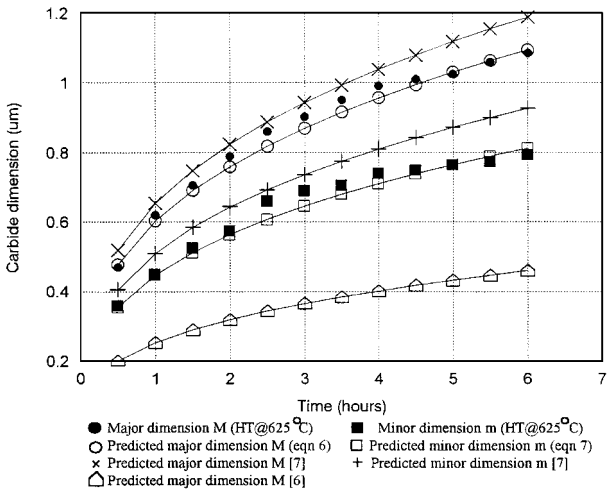

Figure 13 Comparison of growth model produced in the present work, Equations 6 and 7, with other published models.

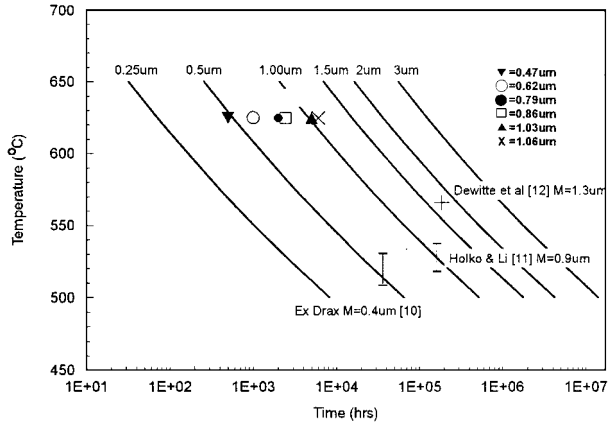

Figure 14 Iso-geometric contours generated using Equation 6 with published data for service Type I carbide size added for comparison.

of the components service temperature. Equation 6 has been used to generate a number of iso-geometric curves for Type I carbides at temperatures ranging from 500 to 700°C and for times in excess of 10,0000 hours, Fig. 14. Superimposed on this predictive plot are experimental observations at 625°C from this programme. As expected, the points fall into the appropriate size band for each time/temperature condition. To evaluate the accuracy of the predictions, published data on Type I carbide sizes from ex-service welds have been included in Fig. 14 [10–12]. These data points also fall close to the appropriate iso-geometric curve. The agreement demonstrated indicates that such an approach may be used to predict the Type I carbide dimensions for a service weld exposed at operating temperatures for a prolonged period. Conversely, for a selected weld with the known service life, Type I carbide size measurements can be used to give an assessment of operating temperatures.

In addition, it was seen that laboratory ageing at 625°C and creep exposure at 590, 605 and 625°C have generated carbides of a similar character to those found in service after 160,000 hours at 538°C [11]. Type I carbides have also been linked to the low ductility failures of nickel based welds in service [13]. It has been suggested that the Type I carbides act as nucleation sites for creep cavities and thus the development of a critical carbide size to nucleate cavities would be important in the life assessment of components. Accurate growth models could be used to assess the service life available to a component before a critical size is developed and subsequent cavitation and cracking occurs.

Similar relationships can be developed between Type I carbides densities and spacing and the observations from service welds in plant. Suggestions have been made that these measurements are critically important to the life assessment of a weldment [7]. Analysis of the number of carbides per unit length on the plane adjacent to the interface shows that the carbides grew relatively quickly early in life and then reach a maximum after about 2000 hours. The number of carbides was then seen to reduce. This can be related to the fact that initially the number of carbides increases and reaches a point where they become close together and coalesce to form longer elongated particles. This effect was observed during the microscopic examination of

the samples and accounts for the fact that although the carbides continue to grow, the number per unit length decreased and thus the interparticle spacing also decreased. A situation can be envisaged where as particles grow in the major axis and the spacing decreases to a point where Type I carbides link up and a near continuous plane of potential weak, low ductility Type I carbide material developing an the parent metal adjacent and parallel to the weld metal. This would create a weak low ductility region which would fail in a similar manner to that seen in service [13].

4.2. Type II carbides

Type II carbides were seen to dissolve with increasing heat treatment. This can be attributed to the tempering effects of the thermal exposure. The 6000 hour heat treatment had completely removed the lath-type interfacial structures seen in the as-received weldment. Studies have shown that regions of Type II in service exposed welds tend to be free of creep cavitation damage [4]. Thus, this region may be considered creep ductile. Therefore, the removal of Type II structures by thermal exposure may increase creep crack propagation rates in nickel based welds.

4.3. Hardness and chemical analysis

The thermal exposure of 2.25Cr-1Mo parent metal invariably results in softening as a result of the tempering of the ferrite/bainite microstructures present. Comparison of the tempering data obtained in this programme with other published work [7, 14] shows that the 2.25Cr-1Mo as-received parent metal (including PWHT) is generally softer than HAZ regions throughout the tempering regime, Fig. 15. Thus, if hardness measurements of service components are available, a relationship between hardness and operating temperature can be developed which can be used in conjunction with carbide growth observations to provide indications as to the components service exposure.

Microhardness measurements on the other hand can be linked to localised changes in microstructure and chemistry. Definite peaks are visible in Fig. 9 which are located at the weld interface and which increase in size with increase thermal exposure. These peaks coincide with the development of extensive Type I carbide array with are co-located with the hardness peaks. This would indicate that the carbides, generally identified as $M_{23}C_6$ and M_6C [15], are developing to an extent where they can be detected by microhardness testing. In addition to peaks, soft regions were detected in the HAZ adjacent to the interface. Nath [16] demonstrated that variations in carbon content were detectable in region adjacent to the weld interface in both the parent HAZ and weld metal regions. A peak of 5 times the base carbon level was detected in nickel based transition joint in the HAZ adjacent to the interface which could account for the peaks in hardness. Also a trough which reduced the carbon content to 50% that of the base level was noted in the HAZ. Again, this could account for the steep drop in HAZ hardness away from the interface peak. Nath also details the variation in chromium and nickel levels at the interface and adjacent regions. These are in good agreement with those observed in the as-received and 6000 hour heat treated weldments and thus the variation of values of these elements does not appear to change greatly with thermal exposure. Thus, a model which determines thermal exposure and subsequent carbide development based on chemical analysis would be best based on the variation in carbon content in a narrow region ($\pm 200\,\mu$m) adjacent to the weld interface rather than a more coarse analysis of other elements near the weld interface.

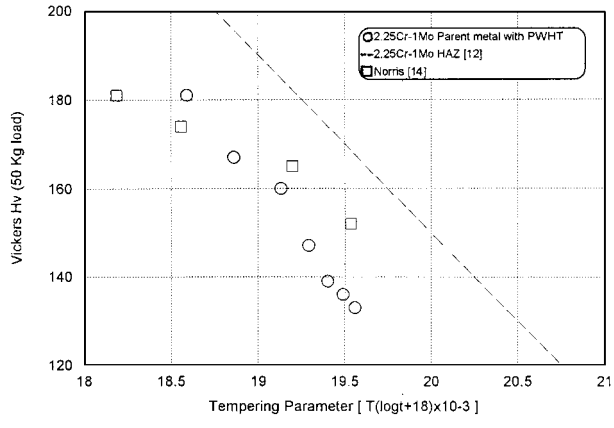

Figure 15 A comparison of tempering performance with data from published sources.

5. Conclusions

Detailed examination of sections of nickel based transition joint from both furnace heat treated and interrupted uniaxial creep specimens has shown that:

1) Furnace heat treatment was successful in developing interfacial carbide structures which were representative of those seen in service welds, ie. Type I and Type II carbides.

2) Ageing caused the Type I carbides to grow and to take on a lenticular morphology. Type II carbides dissolved with increasing thermal exposure.

3) Type I carbides grew along the weld interface and eventually showed evidence of linkage to form continuous regions of carbide structure.

4) Similar microstructural observations were seen in furnace heat treatments and interrupted uniaxial cross weld specimens. Thus, an applied stress leading to local deformation did not appear to change the rate of carbide growth.

5) A simple cubic growth model was developed which accurately described the growth of Type I carbides in heat treated and interrupted creep specimens.

6) By comparison with plant data, it was seen that the model above was able to accurately predict the size of Type I carbide which develop in service. This suggests that the laboratory data generated in times up to 6000 hours at 625°C is relevant to very long term service at 540°C.

Acknowledgements

This work was funded within the HSE-IMC programme on nuclear safety research. Dr. R. Hales and

Dr. D. Miller of Nuclear Electric plc are thanked for their technical contributions.

References

1. D. I. ROBERTS and R. VISWANATHAN, in Proceedings: Seminar on dissimilar welds in fossil-fired boilers, edited by R. Viswanathan, EPRI CS-3623 (1985) p. 1.
2. BS 2633:1987, British Standard Specification for Class I arc welding of ferritic steel pipework for carrying fluids. British Standards Institute.
3. J. D. PARKER and G. C. STRATFORD, "The high temperature performance of nickel based transition joints - Part a: creep deformation," to be published.
4. C. C. LI, in Proceedings: Seminar on dissimilar welds in fossil-fired boilers, edited by R. Viswanathan, EPRI CS-3623, 1985, p. 1.
5. R. J. GRAY, J. F. KING, J. M. LEITNAKER and G. M. SLAUGHTER, *Microstructural Science* **5** (1977) p. 115.
6. R. D. NICHOLSON, *Metals Technology* **11** (1984) 115.
7. R. VISWANATHAN, J. R. FOULDS and D. I. ROBERTS, in Conf. Proc. Boiler tube failures in fossil power plants, EPRI, Atlanta USA, 1987, edited by B. Dooley and D. Broske.
8. C. WAGNER, *Z. Electrochem.* **65**(7&8) (1961) 581.
9. I. M. LIFSHITZ and V. V. SLYOZOV, *J. of Phys. Chem. Solids* **19**(1&2) (1961) 35.
10. DR. R. HALES, Private communication.
11. K. H. HOLKO and C. C. LI, in Proc. Int. Conf. on Welding Technology for Energy Applications, Gatlingburg, Tennesse, 1982, p. 641.
12. M. DEWITTE, L. VERELST and D. THOMAS Jr. R., Presented at 1994 Pressure Vessels and Piping Conference, Minneapolis, June 1994, PVP Vol. 288, edited by W. H. Bamford, p. 243.
13. R. D. NICHOLSON, *Mat. Sci. and Tech.* **1** (1984) 227.
14. S. D. NORRIS, PhD thesis, University of Wales Swansea, 1995.
15. R. D. NICHOLSON, *Materials Science and Tech.* **2** (1986) 686.
16. B. NATH, in Proc. Int. Conf. on Creep Fracture of Engineering Materials and Structures Part II, edited by B. Wilshire and D. R. J. Owen (Pineridge Press, 1984) p. 827.

Received 2 July
and accepted 19 August 1999